Low-cost biomonitoring and high-resolution, scalable models of urban metal pollution

Mathis Loïc Messager, Ian P. Davies, Phillip S. Levin

Low-cost biomonitoring and high-resolution, scalable models of urban metal pollution

Authors

Mathis L. Messager [a] *, Ian P. Davies [a], Phillip S. Levin [a, b]

Affiliations

[a] School of Environmental and Forest Sciences, University of Washington, 3714 Garfield Place, NE, 98195 Seattle, Washington, United States of America

[b] The Nature Conservancy, 74 Wall Street, 98121 Seattle, Washington, United States of America

NE, 98195 Seattle, Washington, United States of America

* Current addresses: Department of Geography, McGill University, Burnside Hall Building, 805 Sherbrooke Street West, Montreal, Quebec H3A 0B9, Canada; and National Institute for Agricultural and Environmental Research (INRAE), 5 rue de la Doua, CS 20244, 69625 Villeurbanne Cedex, France.

Corresponding author**:** Mathis Loïc Messager (messamat@uw.edu)

Other email addresses: ipdavies@uw.edu, pslevin@uw.edu

Keywords

air pollution, stormwater pollution, automobile traffic, PM2.5, moss, Puget Sound

Abstract

As the global toll on human lives and ecosystems exacted by urban pollution grows, planning tools still lack the resolution to identify priority sites where toxic pollution can be most efficiently averted at a spatial scale that matches funding and management. Here we tackle this gap by demonstrating novel scalable methods to monitor and predict urban metal pollution at high resolution (< 5 meter) across large areas (10,000-100,000 km^2) to guide pollution reduction and stormwater management. We showcase and calibrate predictive models of Zn, Cu, and a synthetic index of pollution for the Puget Sound region of Washington State, U.S., a densely urbanized yet important ecosystem of conservation interest, and exemplify their transferability across the entire United States. We leveraged widely and freely available datasets of car traffic characteristics and land use as predictor variables and trained the models with biological monitoring data of metal concentrations in epiphytic moss from > 100 trees based on new rapid and low-cost protocols introduced in this study. Our model predictions, showing that 50% of the total Cu and Zn pollution across the Puget Sound watershed is deposited over only 3.3% of the land area, will allow cities to effectively and efficiently target toxic hotspots.

1. Introduction

The global expansion of urban areas over the past century has led to widespread pollution, yielding a cascade of impacts on ecosystems and human health [1–4]. Car ownership underlies much of this impact as the world's fleet continues growing, exceeding one billion vehicles in 2015 [5]. Ambient air pollution is now considered one of the leading causes of premature death [6–8]. Additionally, precipitation flowing over impervious surfaces transfers a complex mixture of contaminants to streams and waterbodies — metals, polycyclic aromatic hydrocarbons (PAH), pesticides and other pollutants emitted by urban activities are washed off from streets and parking lots or leached from roofs and other construction material by stormwater runoff and subsequently carried into nearby ecosystems [9]. This stormwater runoff is the fastest growing source of water pollution in many areas [10]. With nearly 80% of the population of the world projected to live in cities by the end of the 21st century [3], and the number of vehicles expected to double or triple by 2050 [11], it is imperative to tackle the negative effects of urban dwelling.

Metals are among the pollutants of highest concern in urban areas due to their persistence, bioavailability and toxicity [12–14]. High concentrations of metals threaten aquatic ecosystem functioning and biodiversity, as well as human health [10,15]. In cities, metals are commonly reported pollutants, reaching waterways directly through atmospheric deposition and indirectly through rain runoff by being leached or picked up as dust after depositing and building up on impervious surfaces [16]. Road dust naturally contains metals from eroded soil but anthropogenic sources like building and road materials, vehicle brake, tire wear, and tailpipe emissions are the main non-point sources of metal pollution in urban areas [17–19].

High-resolution estimates of pollutant sources are required to mitigate exposure to toxic compounds by identifying the specific locations and associated site characteristics where the deposition of metals is greatest [20]. Pollution predictions must also be available for large geographic areas to match the spatial scale of funding, management, and some environmental issues [8]. Low-resolution (coarse) models cannot identify emission hot spots, as pollution sources are averaged over large spatial units of analysis, and models developed for small spatial extents may not match the ecological scale relevant to species targeted by management [10]. However, the few models that focus on metals usually lack the combination of resolution and scale for this purpose (but see [21–23]). Therefore, high-resolution, scalable models that describe the relative magnitude of metal pollution sources across space are needed to guide investments across large areas.

Further complicating the training and validation of high-resolution models of urban metal pollution is the dearth of monitoring data at the appropriate temporal and spatial scales. For stormwater management, infrastructure siting requires long-term average metal emission measures in flowing and standing water bodies, yet common monitoring data usually represent snapshots in time subject to high sub-daily, daily, and seasonal variability [24]. Air quality monitoring networks, on the other hand, measure the concentration of metals in Nfine (< 2.5 μm diameter – $PM_{2.5}$) and coarse (2.5–10 μm diameter – PM_{10}) particulate matter [25–27] through costly protocols. Consequently, the geographic density and temporal grain of metal pollution monitoring is currently insufficient to train fine scale models of pollution, and most developing countries lack the resources to install such monitoring infrastructure. Affordable approaches to assess metal pollutant emissions integrated over long time periods thus hold the potential to

greatly facilitate air pollution and stormwater management across large spatial scales and in areas with limited resources[28,29].

The aim of this study was to develop scalable methods to monitor and predict urban metal pollution at high resolution to guide pollution reduction and stormwater management. Here, we showcase and calibrate these methods for the Puget Sound region of Washington State, U.S., a densely urbanized yet important ecosystem of conservation interest [30]. We modeled long-term average pollution levels for two metals of concern, Zn and Cu, as well as a pollution index combining the pollution levels of these two metals with Pb. The model was trained with an extensive set of passive biological monitoring data. We measured metal concentrations in epiphytic moss collected by in-situ portable X-Ray Fluorescence (XRF) spectroscopy for > 100 trees based on new protocols introduced in this study. Lastly, we exemplify the utility of the models by assessing its ability to predict metal air pollution across the U.S.

2. Materials and Methods

2.1. Overview

We first compiled spatial data for six of the main variables that have been reported to drive the spatial distribution of urban metal pollution [31–35]: land use; motor vehicle traffic volume, speed, and congestion; road gradient; and over-ground public transit frequency (TOC.1). Second, we generated pollution source "density maps" that simulate the cumulative and diffuse emissions from each road-based source of pollution (TOC.2). In these source maps, each location is assigned the distance-weighted sum of the value of the variable (e.g. traffic volume) across the entire area within a buffer around that location. This allowed us to account for the cumulative

effect of the variable from multiple roads around every location while accounting for pollution concentrations decay away from each road. Third, we measured the concentrations of metals in epiphytic moss at 87 sites across the greater Seattle area (WA, U.S.) using portable XRF (TOC.3). Fourth, a set of multiple regression models were developed using the density maps values and land use at the sampling sites as candidate predictor variables and the XRF measurements as response variables (i.e. training data, TOC.5). Three models were developed separately for Zn, Cu, and the synthetic pollution index (PI). Zn, Cu, and Pb were selected as our pollutants of study as these elements are among the most commonly studied and reported metal pollutants in urban environments [36–38]. Zn and Cu, in particular, are closely associated with automobile traffic volume and congestion through the emission of rubber tire dust and brake wear dust, respectively [18,37]. The three trained models were subsequently used to make spatially continuous predictions of the relative concentrations of each pollutant across the entire study area (TOC.6). Lastly, we predicted Zn pollution around every air quality monitoring station from the United States Environmental Protection Agency (EPA) that recorded ambient air concentrations of Zn in the form of fine particulate matter (TOC.7). This allowed us to assess how well our predictions fit standard measurements of long-term average air pollution. See Appendix 1 for a detailed description of the methodology and data sources.

2.2. Study area

The Puget Sound region encompasses 41,500 km^2 of upland, freshwater, estuarine and marine habitats, and currently supports a large and increasingly urban population from Vancouver, British Columbia (Canada) to Olympia, Washington (U.S., Fig. 1). Population projections suggest that human numbers in the greater Puget Sound region will increase by two

131 million in the next 30 years, and Seattle, Washington, the largest city in the region, is one of the
132 fastest growing in the country [39]. With over 40 species of birds, mammals, fishes, plants and
133 invertebrates currently listed as threatened, endangered, or as candidates for state and federal
134 endangered species lists, Puget Sound is considered a "hot-spot" of extinction risk [30].
135 Importantly, some of these imperiled species, such as Chinook salmon
136 (*Onchorhynchus tshawytscha*) and killer whales (*Orcinus orca*), are regional icons that have
137 been commemorated in art, culture and tradition for millennia (e.g. [40]).
138
139 *2.3. Candidate predictor variables: data sources and pre-processing*
140 We used the Percent Developed Imperviousness dataset from the 2016 Multi-Resolution
141 Land Characteristics Consortium's National Land Cover Data (NLCD, spatial resolution of 30 m)
142 [41] as a continuous measure of land use intensity. Because the effects of urban land-use on air and
143 water pollution are diffuse, two spatially smoothed imperviousness layers were also generated
144 from this dataset with 3x3 pixel mean and median filters.
145 A single spatial road network dataset with traffic volume (Annual Average Daily Traffic)
146 and speed was compiled from the U.S. Department of Transportation (DOT) and the U.S. Census
147 Bureau (Table S1). The slope of each road segment in the network was calculated from the 3D
148 Elevation Program Digital Elevation Models (Table S1) at the highest resolution available for
149 every location by first smoothing the elevation dataset and then computing the ratio of each road
150 segment's elevation range and length. To quantify traffic congestion, we computed the average
151 traffic flow across the area of interest based on data from the Bing™ Maps REST Services
152 Application Programming Interface (API). To do so, we built a custom tool similar to Tostes and
153 colleagues' [42]. We applied our tool to obtain traffic conditions throughout the Puget Sound

154 watershed area from November 28th, 2018 at 08:00 am to December 5th, 2018 at 08:00. For Air
155 Quality Monitoring Stations, the tool was run from April 9th at 18:00 2019 to April 16th at 18:00
156 2019, resulting in 169 hourly snapshots.
157 Maps of over-ground public transit frequency were generated for the Puget Sound
158 watershed and within the vicinity of Air Quality Monitoring Stations based on static General
159 Transit Feed Specification (GTFS) data from the National Transit Map (Table S1) — the largest
160 seamless compilation of GTFS data in the U.S. at the time of this study. The result provided us
161 with a single seamless layer of the average weekly number of times that a public transit vehicle
162 went through every location across the landscape, thus integrating across all agencies, modes of
163 transport, routes, and schedules.
164
165 *2.4. Pollution spread models*
166 To simulate the spread of pollutants away from roads and thus the cumulative pollution
167 from multiple roads, we generated pollution source density maps of public transit frequency,
168 road gradient, and traffic volume, speed and congestion. For each density map, the value at each
169 location was calculated as the distance-weighted sum of all pixel values within a maximum
170 distance from that location, whereby the weight attributed to each pixel was determined by a
171 distance-decay function. To encompass various possible rates and functional forms of metal
172 particle deposition, we generated 24 candidate density maps for each of these five road-based
173 variables based on a set of 24 different distance-decay functions, each function illustrating a
174 different hypothesized pattern and distance of pollution spread (see Appendix 1). The resulting
175 120 continuous maps of pollution sources were subsequently used as candidate predictor
176 variables to select and train the models of metal pollution across the Greater Seattle area.

177

178 *2.5. Data collection and model training*

179 We used the elemental composition of epiphytic moss on trees from 87 sites determined
180 by portable XRF to train and validate our predictive models of pollution (Fig. 1, see Appendix 1
181 and [Messager et al. companion paper] for more information on sampling design and protocols).
182 Mosses have been widely used in Europe as biological monitors of metal pollution for decades,
183 because they readily accumulate pollutants over time, reflecting long term pollution levels [43,44].
184 Unlike plants, they lack roots and a cuticle, so they absorb nutrients from the atmosphere over
185 their entire surface and all cells are directly exposed to wet deposition [45]. Pollutants in dust also
186 accumulate on their surface through dry deposition [46]. Their high cation exchange capacity
187 results in moss cells passively trapping pollutants, including metals [45]. As a result, mosses more
188 readily accumulate atmospheric metals than vascular plants, and metal concentrations in moss
189 pseudo-tissues are not as influenced by local variations in soil metal levels [29,47]. In addition,
190 mosses are ubiquitous in the study region, in both rural and urban settings, and persist even in the
191 most polluted urban sites. Leveraging these characteristics, multiple studies have successfully
192 used elemental analysis of mosses to assess the spatial distribution and sources of urban and
193 motor vehicle traffic-related metal pollution with high specificity [28,31,48].

194

195 For this study, a new protocol of rapid in-situ elemental analysis by portable XRF was
196 developed. With this method, photons are emitted from an X-ray tube in a portable instrument
197 whose measuring window is directly applied against moss mats growing on tree bark. The
198 emitted photons interact with the atoms within the moss sample, which in turn emit photons at
199 energy levels that are specific to each element. Photons from the moss atoms are then received,

counted, and converted by the instrument into a spectrum of energy with clearly identifiable peaks whose size reflects the relative quantity of each element in the sample [49]. Portable XRF is now a common tool whose performance is comparable to more conventional methods like benchtop XRF and inductively-coupled plasma-optical emission spectrometry (ICP-OES) for the analysis of hazardous metal concentrations in soils and plants [50–52]. We show in [Messager et al. companion paper] that, compared to quantitation by ICP-OES, pXRF enables quantitative screening of Cu (pseudo-R^2 = 0.75) and Zn (pseudo-R^2 = 0.81), and qualitative screening of Pb (R^2 = 0.63), with high measurement replicability. While epiphytic moss has previously been used for urban metal pollution mapping [28], this is, to the authors' knowledge, the first time that portable XRF was used for biological monitoring of fine-scale spatial patterns in ambient metal pollution.

Although 87 different sites were selected for sampling, measurements were separately taken from two closely adjacent trees in a quarter of the sites to assess small-scale variations in metal concentration. Moss mats were thus sampled on a total of 109 trees (measurements from single trees, rather than sites, are hereon used as our unit of analysis). Sampling took place in July-August 2018 and March-April 2019. As various studies have shown that air-moss metal concentration relationships vary among species [53], measurements were taken from a single moss species, *Orthotrichum lyelli* Hook. & Taylor growing on hardwood tree species. Portable XRF assays were obtained from three different moss mats on each tree using a Bruker Tracer III-SD (T3S2606, Bruker Elemental, Kennewick, WA, U.S.). Spectral data were processed and normalized to yield a comparable 'concentration' index across samples using standard analysis protocols (See Appendix 1 and [Messager et al. companion paper] for details on the protocol) [51].

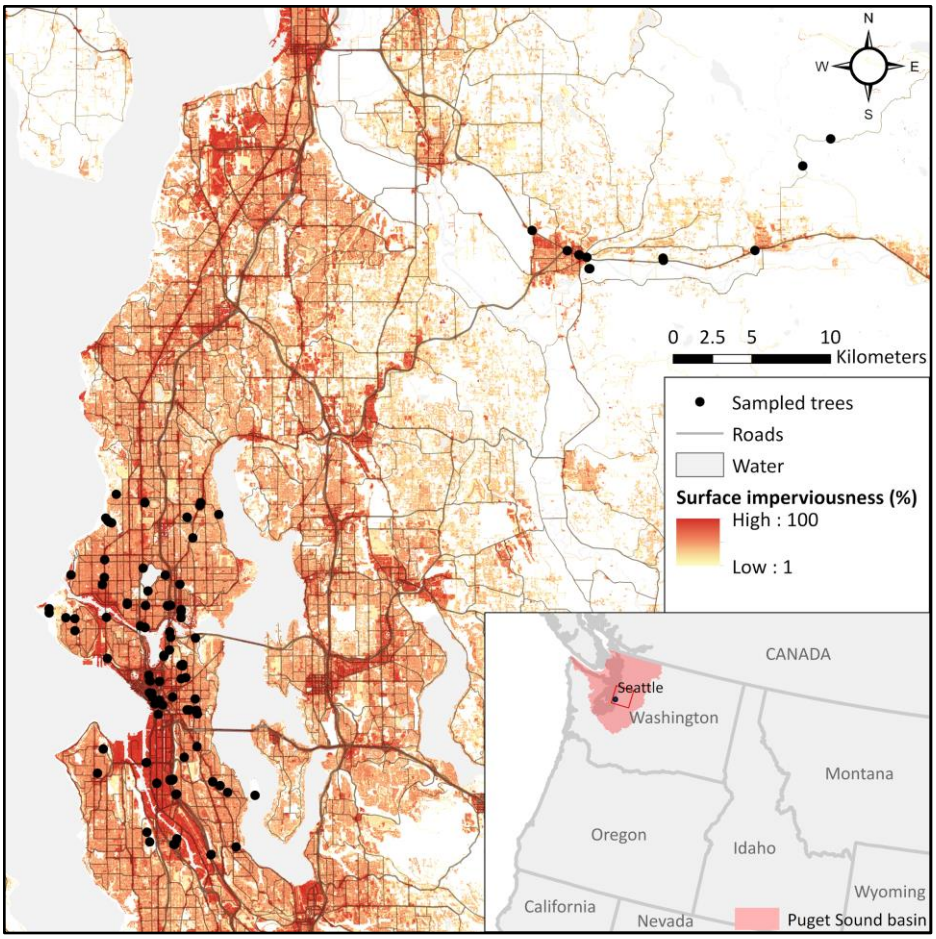

Figure 1. *Spatial distribution of sampled trees used in model development (black points, after outlier removal: n = 107), roads (grey lines, excluding local roads) and surface imperviousness (National Land Cover Dataset 2016) across the Greater Seattle area (Washington State, U.S.), the most densely urbanized region of the Puget Sound watershed (pink polygon in inset map).*

[1.5 column-fitting image]

We developed three separate models for Cu, Zn, and a pollution index. These multiple regression models were developed through model selection [54], all using the density map values and imperviousness at the sampling sites as candidate predictor variables and the element concentrations as response variables (see Appendix 1 for a detailed description).

The pollution index was computed with the following equation for each sampled tree *i*:

$$Pollution\ index_i = \left(\frac{[Cu]_i}{[Cu]_{ref}} \times \frac{[Pb]_i}{[Pb]_{ref}} \times \frac{[Zn]_i}{[Zn]_{ref}}\right)^{1/3} \qquad \textit{(Equation 1)}$$

Where $[Element]_i$ is the element's normalized net count rate averaged over the three XRF assays at that site and $[Element]_{ref}$ is the background normalized net count rate (after within-site averaging) for that element recorded at a reference site away from pollutant sources.

After selecting a reduced set of predictor variables through preliminary selection, a systematic model selection was conducted to develop a multiple regression model for each response variable [54]. We then assessed whether including sampling season (summer 2018 or spring 2019) as a fixed effect improved the model, to take in account the potential influence of temperature and precipitation on moss pollution retention [55–57]. The model residuals were also evaluated for spatially collinearity; we built spatial simultaneous autoregressive error models (linear regression models accounting for spatial error structure) when appropriate [58].

2.6.Model predictions and fit to air pollution measurements

Using the trained models described above, we made spatially continuous predictions of pollution for the Puget Sound region and around every air quality monitoring station operated by the EPA across all states of the contiguous U.S. The latter allowed us to assess whether our estimates of metal concentrations from a model trained with local bio-monitoring data could be related to more standard measurements of air pollution beyond our focal area. We selected all air quality monitoring sites in the conterminous U.S. with at least 200 measurements of Zinc $PM_{2.5}$ ($\mu g/m^3$) from 2014 to 2019 and extracted the Zn concentration estimated by our model (Zn_{pred}) for each of these sites. As spatial and temporal variations in air pollution are strongly influenced by local climatic and meteorological factors, we also computed 37 variables identified as key drivers of $PM_{2.5}$ through 50th percentile quantile regressions by Porter and colleagues [59]. To

assess the adequacy of Zn_{pred} for predicting Zn $PM_{2.5}$ records, we compared two partial least-square regression (PLSR) model of Zn $PM_{2.5}$ (after logarithmic transformation): the first only included meteorological variables as predictors whereas the second included those 37 variables together with Zn_{pred}.

3. Results and Discussion

3.1. Observed distribution and drivers of metal pollution in the study area

XRF assays of epiphytic moss revealed that numerous metals were prevalent throughout the Puget Sound watershed. Their concentrations covaried with urban land use and motor vehicle traffic, often ranging in concentration by an order of magnitude above background levels (Appendix 2). Metals detected by our sampling included Cd, Co, Cr, Cu, Fe, Mn, Ni, Pb, Sr, Ti, Zn, and Zr. Notably, Zn concentration in the most polluted site was 23 times higher than in the most isolated area, whereas Cu varied by a factor of 10 throughout the area. The concentrations of metals measured by XRF sampling also covaried among elements (Appendix 3, Fig. S1). This further justified our focus on a reduced set of elements (Cu, Zn, and Pb) that could serve as indicators for a broader suite of metal pollutants. Clusters of elements revealed common physicochemical properties, patterns of spatial dispersion, and potential sources. High concentrations of Zn, Co, Fe, Zr, Cr, and Ti tended to co-occur ($0.6 < \text{Pearson's } r < 0.9$), Cu exhibiting slightly different distributional patterns, whereas Pb was clustered with As. The observed correlations among metals can be attributed to their co-occurrence in automotive parts and in crustal dust, as traffic leads to non-exhaust emissions through both abrasion (i.e. of brake pads and tires) and dust resuspension[18,60].

Applying our rapid and low-cost biomonitoring protocol across a dense array of sites, and combining these measurements with widely available spatial data on potential pollution sources, allowed us to shed light on the traffic and land use characteristics most responsible for the occurrence of different metals in urban environments. This analysis showed for example that Zn and Cu concentrations are both strongly correlated with traffic speed ($r > 0.5$). Zn also strongly covaries with traffic volume and congestion ($0.6 < r < 0.7$) whereas Cu is correlated with bus transit volume ($r > 0.6$, Appendix 3, Fig. S2). The distance-decay functions used to produce the density maps of pollutant predictors that were most correlated to metal concentrations further hinted at the relative distances to which different metals disperse away from their source of emission. For instance, Zn is slightly more correlated to traffic speed and volume density maps generated with 100 m kernels compared to those based on 200 m kernels or larger. On the other hand, Cu is most correlated to density maps produced with the largest kernels of dispersion for every pollution predictor. Closely associated with tire wear, Zn in dry deposition is usually associated with larger particle size (> 10 µm) whereas Pb, Cd, Ni and Cu are mostly present in smaller particle sizes (< 10 µm) [37]. As particles < 10 µm behave more like gases, diffusing along concentration gradients to deposit on surfaces, they tend to travel further than coarser particles whose deposition rates are more gravity-driven, explaining the differences in spread patterns we observed between Cu and Zn [61].

3.2. Model training and validation results in the Puget Sound watershed

The models of pollution developed here — for Zn, Cu, and a pollution index — relied on only two to three predictors each, and all yielded estimates with average percentage errors from 20 to 30% (Fig. 2). These three models explained 65%, 64% (78%) and 57% (72%) of the

variability in Zn, Cu, and pollution index across sampled sites, respectively, based on pseudo-R^2 computed with (and without) outliers (Fig. 2). For a full list of candidate models, performance and diagnostic tests, refer to Appendix 4. To achieve normality and homoscedasticity of residuals, the regression models of Cu and pollution index were trained without outliers (grey points in Fig. 2 scatterplots). Sampling season did not have a significant effect ($p > 0.05$) in the models. Regression coefficients from autoregressive error models with inverse distance spatial weight matrices based on one nearest neighbor were used for model predictions in all three cases, as Lagrange Multiplier robust diagnostic tests revealed spatial error dependence in the initial simple linear regression models. The metal pollutant concentrations were thus estimated according to the following regression models (based on Zn and Cu values maximum-standardized to 100):

$$Zn = exp(2.042 + 0.417 \cdot volume_{log100}^{1/4} + 0.012 \cdot imperviousness_{smooth}) \text{ (Equation 2)},$$

$$Cu = 17.522 + 5.808 \cdot transit_{log200}^{1/2} + 0.142 \cdot imperviousness_{smooth} \text{ (Equation 3)},$$

$$Pollution\ index = 1.783 + 0.048 \cdot volume_{log100} + 1.690 \cdot transit_{linear100}^{1/3} + 0.031 \cdot imperviousness_{smooth} \text{ (Equation 4)},$$

where $volume_{log100}$ is the value from the density map of average annual daily traffic created with a 100 m-log kernel, $transit_{log200}$ and $transit_{linear100}$ are produced with bus transit density maps with 200 m-log and 100 m-linear kernels, respectively, and $imperviousness_{smooth}$ is based on a 3x3 median filter of imperviousness.

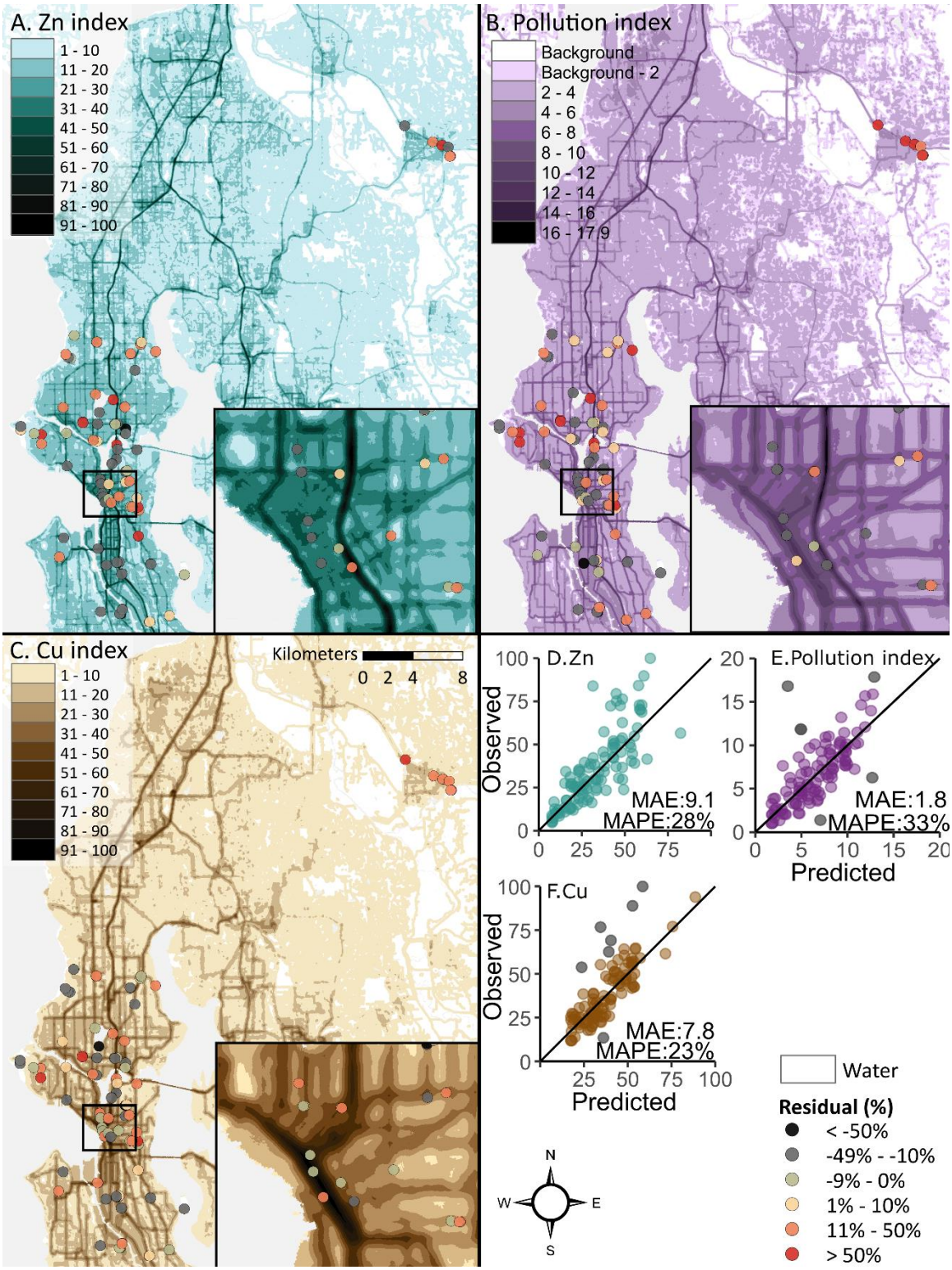

Figure 2. *Prediction maps and scatterplots of observed vs. predicted metal pollution for (A, D) Zinc, (B, E) Pollution index, and (C, F) Copper (respectively). Map values for Zn and Cu are*

minimum-maximum standardized to describe the spatial distribution of metal concentrations across the area, 0 reflecting "background" metal concentrations presumably due to local crustal deposits at the least impacted site, and 100 corresponding to the highest predicted value across the Puget Sound watershed. For all models, Mean Absolute Percentage Error (MAPE) and Mean Absolute Error (MAE, of the standardized indices) were below 30% and 10, respectively. Residuals show percentage error of predictions at sampled sites based on XRF-measured metal pollution. Insets show the heavily trafficked downtown area of Seattle adjacent to a section of the Interstate Highway 5 where a dense array of measurements were conducted.

[2 column-fitting image]

Our results echo previous studies relating motor vehicle traffic characteristics with measured air, soil, and stormwater pollution. Horstmeyer and colleagues [32], for instance, document the greatest Pb, Zn, and Cu concentrations in the topsoil of vegetated infiltration swales at sites with high traffic volume or with frequent braking and acceleration, at crossings, roundabouts and in stop-and-go traffic. Cu and Zn concentrations in mosses along transects of nine roads also increased with traffic density and the incline of the roads in Austria [31]. While additional predictors could have been added to increase the performance of our model, we instead focused on using widely available, free-to-access data to maximize the scalability of our model and its transferability to varied geographical contexts. The fact that our models including bus transit best predicted Cu was a surprising finding, but we conjecture that bus transit routes reflect major transportation axes also used by heavy commercial motor vehicles (i.e. trucks) and thus buses do not solely account for the pollution patterns. Pb was not as well predicted by traffic and land use as Zn and Cu. This lower predictive ability goes against our expectations as Pb,

349 despite having been phased out of gasoline for several decade, remains a prevalent component of
350 motor vehicle parts [18,62]. Point-source pollution spreading over large distances and the age of
351 surrounding buildings may be more strongly driving the spatial distribution of this pollutant [63].
352 For the development of more local models, we therefore posit that additional sources of metal
353 pollution to account for, when available, should include: heavy-duty motor vehicle traffic [32],
354 building density and age [63], parcel-level land use (e.g. parking lots [32]), road surface material [64],
355 commercial railways [65], and locations of point-source pollution [28].
356
357 *3.3. Model transferability: comparison to nationwide monitoring data*
358
359 Although our models were trained with metal concentrations in epiphytic moss from across
360 the Puget Sound watershed, they could also predict air metal pollution at the continental scale
361 with relative accuracy. Together with long-term meteorological and climatic predictors, our
362 estimates of Zn pollution explained 59% of the variability in long-term average Zinc $PM_{2.5}$
363 ($\mu g/m^3$) across all 195 air quality stations with at least 200 daily observations (2014-2019) across
364 the U.S. (Fig. 3). Here we focused on assessing the ability of our models to predict Zn in fine
365 particulate matter ($PM_{2.5}$). However, Zn, Cu and Pb emissions are associated with a range of
366 particle sizes that might be better predicted by our model (e.g. PM_{10} and coarser [18,66]). In
367 addition, although the goal of our US-wide analysis was to assess the relevance of our model
368 estimates regarding long-term air metal pollution, more complex models accounting for temporal
369 (weekly and seasonal) and spatial autocorrelation could achieve greater predictive ability.
370

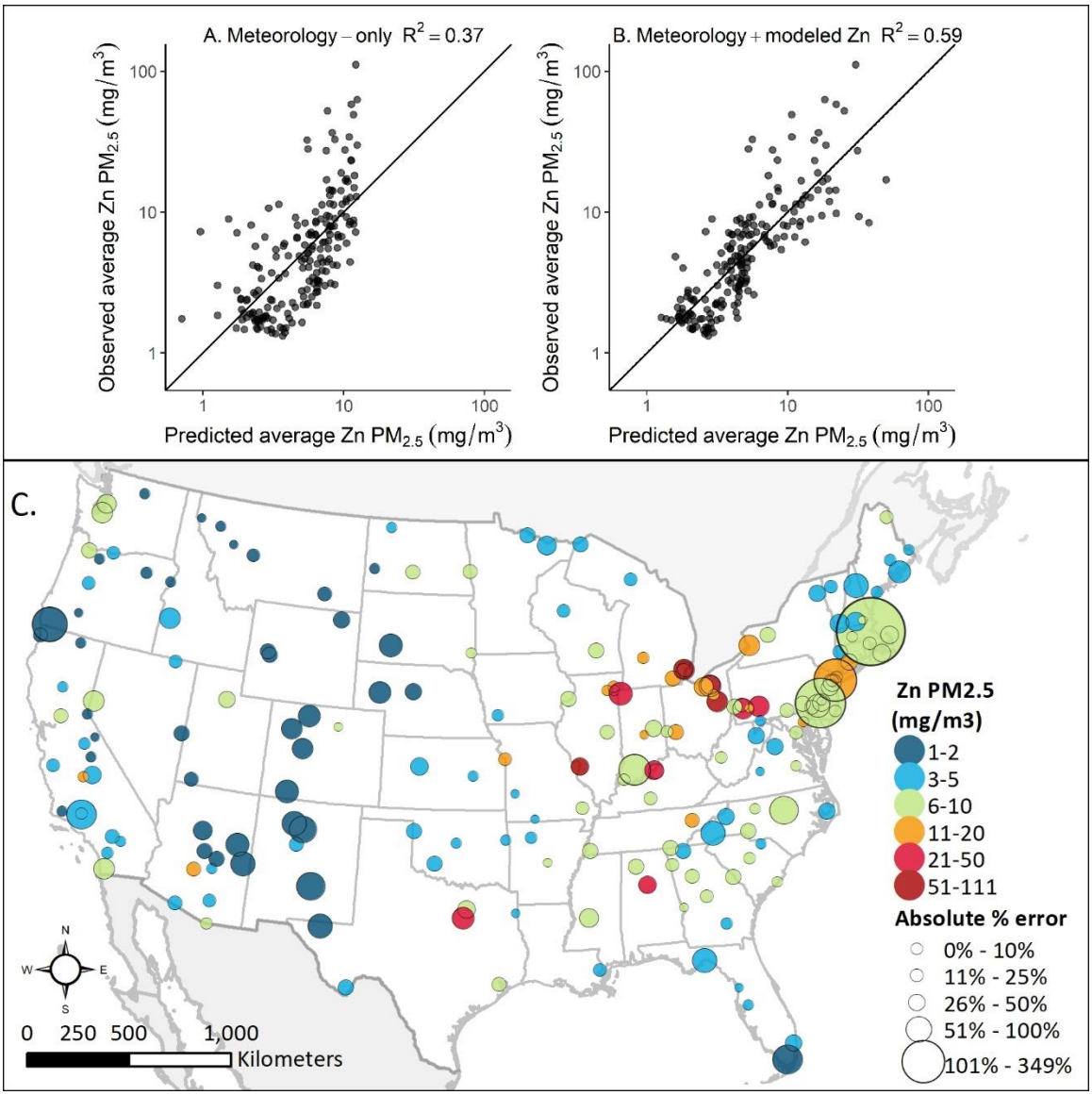

371

372 ***Figure 3.*** *Predictive performance of (A) a meteorology-only partial least-square regression*
373 *(PLSR) and (B) a PLSR combining meteorological variables and the Zn index estimated by the*
374 *model developed in this study as predictor variables for (C) long-term average Zn* $PM_{2.5}$ *(color,*
375 mg/m^3*) recorded at 195 air quality stations across the United States from 2014 to 2019. The*
376 *black diagonal lines (A and B) are 1:1 lines. The points in the map (C) are sized according to the*
377 *absolute percentage error of the [meteorology + modeled Zn] PLSR relative to measured Zn*
378 $PM_{2.5}$ *at the stations.* **[2 column-fitting image]**

The biomonitoring method and modelling framework demonstrated here provide a unique combination of scale and resolution. They can be leveraged for fine-scale decision-making to control a family of pollutants that is rarely modeled yet whose threat to the environment is increasingly recognized [10]. A large portion of urban metal pollution is initially emitted, or resuspended, to the atmosphere before settling on the road surface and being washed off by stormwater[35,67,68]. Therefore, moss biomonitoring and the associated predictive models can inform stormwater management in identifying hot spots of metal emission by these sources located upstream from waterbodies of interest. Although moss has been used across Europe to map large scale patterns of pollution [69], only a handful of studies have demonstrated the use of bryophytes for assessing fine scale patterns of pollution [31]. Using portable XRF, we were able to assess the concentration of 12 metals across 87 sites in about five minutes at each location, allowing for fine-scale assessment of the spatial distribution of pollution. By contrast, there are only two stations with long-term Zn $PM_{2.5}$ data in the Puget Sound watershed. The models can also be further adapted with moss measurements from other locations of interest. Because we trained our models based on widely and freely available datasets of pollution predictors, this framework can be leveraged to estimate metal pollution at high resolution (here ~ 5 m) in other contexts and across large areas. Outside of the United States for example, the road network from the Open Street Map dataset, a global crowd-sourced collaborative mapping project, is nearly complete [70], and our novel tool for assessing the degree of traffic congestion using Bing ™ could be applied in > 70 countries at the time of this study [71]. Traffic congestion data could also be more easily obtained through the establishment of custom user agreements with companies specializing in the collection of traffic data (e.g. INRIX®). Lastly, sub-models and variable

substitution can be used to accommodate cases where predictor variables may be unavailable (e.g. traffic volume) as multiple variables performed well in predicting pollution (Appendix 4).

3.4. Sources of errors and uncertainty

Multiple sources of uncertainty are associated with the framework introduced here, stemming from the use of moss biomonitoring, XRF measurements, as well as in the predictor variable data. The main source of uncertainty in moss-based biomonitoring is that metal levels in moss pseudo-tissue do not reflect a passive and steady accumulation over time but a dynamic equilibrium between concentrations in the environment, moss growth, and meteorology [53]. We review sources of uncertainty in moss measurements in Appendix 5, including precipitation, proximity to saltwater, pseudo-tissue age and growth rate. Field sampling was conducted across two different seasons due to maintenance requirements for the XRF instrument — while we did not find a significant effect of season in our models, we recommend that future studies conduct all sampling within a single season or re-sample the same sites across different periods of the year to better capture seasonal variability [44]. Due to these uncertainties, moss biomonitoring is best suited for assessing the spatial distribution of pollution in relative terms rather than determining absolute levels for the evaluation of pollution criteria compliance. Regarding field XRF measurements, the main uncertainty resides in the heterogeneity of moss samples growing on trees, resulting in unequal densities of pseudo-tissue and depth of measurements. Nonetheless, the low level of tissue differentiation and the lack of a cuticle greatly reduces variability in XRF measurements of moss compared to vascular plants [51]. One additional limitation of XRF is that the prevalence of some commonly used tracers of non-exhaust traffic pollution (e.g. Sb, Ba[60,72,73]) cannot be accurately determined at the same time as those discussed in this study;

these elements' characteristic energy lines occur outside of the region that the instrument was set to measure (through the use of a yellow filter, see Appendix 1 for details on protocol). Owing to its affordability and speed, the resulting ability to compute averages over replicated measurements, and the minimal disruption of samples involved compared to conventional methods (e.g. sample extraction, transport, processing, digestion), we believe that this protocol is a significant advance towards high resolution monitoring of urban metal pollution.

3.5. Predicted metal pollution across the Puget Sound watershed

With the assurance that our models satisfactorily described the spatial patterns of the three metal pollution indicators, we made predictions of metal pollution across the entire ~40,000 km^2 of the Puget Sound watershed. These estimates show that the pollutant footprint of human development spans across the entire landscape, with 27% of the watershed's land area (excluding all 30x30 m pixels identified as water by the National Land Cover Dataset) exhibiting metal concentrations above background levels for at least one of the indicators. Cu affects the greatest area in the region, as expected from the larger size of the distance-decay function for bus transit (Equation 3) in its computation. Our work also reveals that metal pollution is very localized: 50% of the total pollution deposited on land across the Puget Sound watershed is deposited over only 3.3% of the land area for both Cu and Zn (Fig. 2 and 3).

3.6. Conclusion

Effectively and efficiently combating pollution generated from motor vehicles is a major challenge facing natural resource managers and urban planners. In this study, we demonstrate the utility of new biomonitoring techniques that can provide unique insight into the spatial

447 distribution of pollution sources at a fraction of the cost of usual approaches. Intensive sampling
448 of epiphytic moss with pXRF revealed the existence of Zn and Cu emission hotspots in densely
449 urbanized areas of the Puget Sound watershed with metal concentrations exceeding background
450 levels by an order of magnitude. Combined with open access datasets to train predictive models,
451 our inexpensive, rapid, and rigorous approach allows managers to identify and mitigate toxic
452 metals at fine spatial scales over large geographic regions. Here we applied these models to
453 predict the concentration of metals at ~5 m resolution across the Puget Sound watershed and
454 around every air quality monitoring station in the contiguous U.S. With increasingly limited
455 resources, this new approach holds the potential for cities to target toxic hotspots, thus
456 maximizing environmental returns on mitigation investments.
457
458
459
460

Data availability

All scripts used in this study are available for reuse (https://github.com/messamat/traffic for Bing™ traffic flow analysis, https://github.com/messamat/stormwater_samplingPy for GIS analysis and mapping, and https://github.com/messamat/stormwater_samplingR for sampling, XRF data post-processing, and statistical analysis). All data are also available at [figshare URL].

Acknowledgements

We are grateful to Amir Harding and Luwam Gabreselassie for their great help with field work. We thank Tom Deluca and Amanda Bidwell for initiating this project's methodology and providing us with the XRF analyzing device, The Nature Conservancy in Washington, all of the staff there and in particular the Science and Puget Sound teams, as well as the UW Interdisciplinary and Conservation Science Lab for their support and enthusiasm throughout the project. We also thank Lee Drake for his tutorials and advice on XRF analysis. The manuscript was improved by the insightful comments from Ailene Ettinger.

Funding for this project was generously provided by the Boeing company, the Nature Conservancy of Washington, and the University of Washington School of Environmental and Forest Sciences.

Disclosures

The authors declare no competing financial or other interest.

Associated content

See the accompanying Supporting Information for the full methodology (Appendix 1), a table of the selected measured elemental concentrations and land use characteristics at sites sampled by XRF (Appendix 2), cluster and correlation analysis results depicting the relationships among selected elemental concentrations measured in epiphytic moss by XRF and land use and vehicle traffic pollution predictors (Appendix 3), model development tables (Appendix 4), and a literature review of the sources of uncertainty related to moss biomonitoring of ambient metal pollution (Appendix 5).

References

(1) Seto, K. C.; Fragkias, M.; Güneralp, B.; Reilly, M. K. A Meta-Analysis of Global Urban Land Expansion. *PLoS One* **2011**, *6* (8), e23777. https://doi.org/10.1371/journal.pone.0023777.

(2) Dargay, J.; Gately, D.; Sommer, M. Vehicle Ownership and Income Growth, Worldwide: 1960-2030. *Energy J.* **2007**, *28* (4), 143–170. https://doi.org/10.5547/ISSN0195-6574-EJ-Vol28-No4-7.

(3) Jiang, L.; O'Neill, B. C. Global Urbanization Projections for the Shared Socioeconomic Pathways. *Glob. Environ. Chang.* **2017**, *42*, 193–199. https://doi.org/10.1016/j.gloenvcha.2015.03.008.

(4) Walsh, C. J.; Roy, A. H.; Feminella, J. W.; Cottingham, P. D.; Groffman, P. M.; Morgan, R. P. The Urban Stream Syndrome: Current Knowledge and the Search for a Cure. *J. North Am. Benthol. Soc.* **2005**, *24* (3), 706–723. https://doi.org/10.1899/04-028.1.

(5) Davis, S.; Boundy, R. G. *Transportation Energy Data Book: Edition 38*; United States, 2020. https://doi.org/10.2172/1606919.

(6) Forouzanfar, M. H.; Afshin, A.; Alexander, L. T.; Biryukov, S.; Brauer, M.; Cercy, K.; Charlson, F. J.; Cohen, A. J.; Dandona, L.; Estep, K.; Ferrari, A. J.; Frostad, J. J.; Fullman, N.; Godwin, W. W.; Griswold, M.; Hay, S. I.; Kyu, H. H.; Larson, H. J.; Lim, S. S.; Liu, P. Y.; Lopez, A. D.; Lozano, R.; Marczak, L.; Mokdad, A. H.; Moradi-Lakeh, M.; Naghavi, M.; Reitsma, M. B.; Roth, G. A.; Sur, P. J.; Vos, T.; Wagner, J. A.; Wang, H.; Zhao, Y.; Zhou, M.; Barber, R. M.; Bell, B.; Blore, J. D.; Casey, D. C.; Coates, M. M.; Cooperrider, K.; Cornaby, L.; Dicker, D.; Erskine, H. E.; Fleming, T.; Foreman, K.;

Gakidou, E.; Haagsma, J. A.; Johnson, C. O.; Kemmer, L.; Ku, T.; Leung, J.; Masiye, F.; Millear, A.; Mirarefin, M.; Misganaw, A.; Mullany, E.; Mumford, J. E.; Ng, M.; Olsen, H.; Rao, P.; Reinig, N.; Roman, Y.; Sandar, L.; Santomauro, D. F.; Slepak, E. L.; Sorensen, R. J. D.; Thomas, B. A.; Vollset, S. E.; Whiteford, H. A.; Zipkin, B.; Murray, C. J. L.; Mock, C. N.; Anderson, B. O.; Futran, N. D.; Anderson, H. R.; Bhutta, Z. A.; Nisar, M. I.; Akseer, N.; Krueger, H.; Gotay, C. C.; Kissoon, N.; Kopec, J. A.; Pourmalek, F.; Burnett, R.; Abajobir, A. A.; Knibbs, L. D.; Veerman, J. L.; Lalloo, R.; Scott, J. G.; Alam, N. K. M.; Gouda, H. N.; Guo, Y.; McGrath, J. J.; Jeemon, P.; Dandona, R.; Goenka, S.; Kumar, G. A.; Gething, P. W.; Bisanzio, D.; Deribew, A.; Darby, S. C.; Ali, R.; Bennett, D. A.; Jha, V.; Kinfu, Y.; McKee, M.; Murthy, G. V. S.; Pearce, N.; Stöckl, H.; Duan, L.; Jin, Y.; Li, Y.; Liu, S.; Wang, L.; Ye, P.; Liang, X.; Azzopardi, P.; Patton, G. C.; Meretoja, A.; Alam, K.; Borschmann, R.; Colquhoun, S. M.; Weintraub, R. G.; Szoeke, C. E. I.; Ademi, Z.; Taylor, H. R.; Wijeratne, T.; Batis, C.; Barquera, S.; Campos-Nonato, I. R.; Contreras, A. G.; Cuevas-Nasu, L.; De, V.; Gomez-Dantes, H.; Heredia-Pi, I. B.; Medina, C.; Mejia-Rodriguez, F.; Montañez Hernandez, J. C.; Razo-García, C. A.; Rivera, J. A.; Rodríguez-Ramírez, S.; Sánchez-Pimienta, T. G.; Servan-Mori, E. E.; Shamah, T.; Mensah, G. A.; Hoff, H. J.; Neal, B.; Driscoll, T. R.; Kemp, A. H.; Leigh, J.; Mekonnen, A. B.; Bhatt, S.; Fürst, T.; Piel, F. B.; Rodriguez, A.; Hutchings, S. J.; Majeed, A.; Soljak, M.; Salomon, J. A.; Thorne-Lyman, A. L.; Ajala, O. N.; Bärnighausen, T.; Cahill, L. E.; Ding, E. L.; Farvid, M. S.; Khatibzadeh, S.; Wagner, G. R.; Shrime, M. G.; Fitchett, J. R. A.; Aasvang, G. M.; Savic, M.; Abate, K. H.; Gebrehiwot, T. T.; Gebremedhin, A. T.; Abbafati, C.; Abbas, K. M.; Abd-Allah, F.; Abdulle, A. M.; Abera, S. F.; Melaku, Y. A.; Abyu, G. Y.; Betsu, B. D.; Hailu, G. B.; Tekle, D. Y.; Yalew, A. Z.; Abraham, B.; Abu-Raddad, L. J.; Adebiyi, A. O.; Adedeji, I. A.; Adou, A. K.; Adsuar, J. C.; Agardh, E. E.; Rehm, J.; Badawi, A.; Popova, S.; Agarwal, A.; Ahmad, A.; Akinyemiju, T. F.; Schwebel, D. C.; Singh, J. A.; Al-Aly, Z.; Aldhahri, S. F.; Altirkawi, K. A.; Terkawi, A. S.; Aldridge, R. W.; Tillmann, T.; Alemu, Z. A.; Tegegne, T. K.; Alkerwi, A.; Alla, F.; Guillemin, F.; Allebeck, P.; Rabiee, R. H. S.; Fereshtehnejad, S. M.; Kivipelto, M.; Carrero, J. J.; Weiderpass, E.; Havmoeller, R.; Sindi, S.; Alsharif, U.; Alvarez, E.; Alvis-Guzman, N.; Amare, A. T.; Ciobanu, L. G.; Taye, B. W.; Amberbir, A.; Amegah, A. K.; Amini, H.; Karema, C. K.; Ammar, W.; Harb, H. L.; Amrock, S. M.; Andersen, H. H.; Antonio, C. A. T.; Faraon, E. J. A.; Anwari, P.; Ärnlöv, J.; Larsson, A.; Artaman, A.; Asayesh, H.; Asghar, R. J.; Assadi, R.; Atique, S.; Avokpaho, E. F. G. A.; Awasthi, A.; Ayala, B. P.; Bacha, U.; Bahit, M. C.; Balakrishnan, K.; Barac, A.; Barker-Collo, S. L.; del Pozo-Cruz, B.; Mohammed, S.; Barregard, L.; Petzold, M.; Barrero, L. H.; Basu, S.; Del, L. C.; Bazargan-Hejazi, S.; Beardsley, J.; Bedi, N.; Beghi, E.; Sheth, K. N.; Bell, M. L.; Huang, J. J.; Bello, A. K.; Santos, I. S.; Bensenor, I. M.; Lotufo, P. A.; Berhane, A.; Wolfe, C. D.; Bernabé, E.; Roba, H. S.; Beyene, A. S.; Hassen, T. A.; Mesfin, Y. M.; Bhala, N.; Bhansali, A.; Biadgilign, S.; Bikbov, B.; Bjertness, E.; Htet, A. S.; Boufous, S.;

Degenhardt, L.; Resnikoff, S.; Calabria, B.; Bourne, R. R. A.; Brainin, M.; Brazinova, A.; Majdan, M.; Shen, J.; Breitborde, N. J. K.; Brenner, H.; Schöttker, B.; Broday, D. M.; Brugha, T. S.; Brunekreef, B.; Kromhout, H.; Butt, Z. A.; van Donkelaar, A.; Martin, R. V.; Cárdenas, R.; Carpenter, D. O.; Castañeda-Orjuela, C. A.; Castillo, J.; Castro, R. E.; Catalá-López, F.; Chang, J.; Chiang, P. P.; Chibalabala, M.; Chimed-Ochir, O.; Jiang, Y.; Takahashi, K.; Chisumpa, V. H.; Mapoma, C. C.; Chitheer, A. A.; Choi, J. J.; Christensen, H.; Christopher, D. J.; Cooper, L. T.; Crump, J. A.; Poulton, R. G.; Damasceno, A.; Dargan, P. I.; das Neves, J.; Davis, A. C.; Newton, J. N.; Steel, N.; Davletov, K.; de Castro, E. F.; De, D.; Dellavalle, R. P.; Des, D. C.; Dharmaratne, S. D.; Dhillon, P. K.; Lal, D. K.; Zodpey, S.; Diaz-Torné, C.; Dorsey, E. R.; Doyle, K. E.; Dubey, M.; Rahman, M. H. U.; Ram, U.; Singh, A.; Yadav, A. K.; Duncan, B. B.; Kieling, C.; Schmidt, M. I.; Elyazar, I.; Endries, A. Y.; Ermakov, S. P.; Eshrati, B.; Farzadfar, F.; Kasaeian, A.; Parsaeian, M.; Esteghamati, A.; Hafezi-Nejad, N.; Sheikhbahaei, S.; Fahimi, S.; Malekzadeh, R.; Roshandel, G.; Sepanlou, S. G.; Hassanvand, M. S.; Heydarpour, P.; Rahimi-Movaghar, V.; Yaseri, M.; Farid, T. A.; Khan, A. R.; Farinha, C. S. E. S.; Faro, A.; Feigin, V. L.; Fernandes, J. G.; Fischer, F.; Foigt, N.; Shiue, I.; Fowkes, F. G. R.; Franklin, R. C.; Garcia-Basteiro, A. L.; Geleijnse, J. M.; Jibat, T.; Gessner, B. D.; Tefera, W.; Giref, A. Z.; Haile, D.; Manamo, W. A. A.; Giroud, M.; Gishu, M. D.; Martinez-Raga, J.; Gomez-Cabrera, M. C.; Gona, P.; Goodridge, A.; Gopalani, S. V.; Goto, A.; Inoue, M.; Gugnani, H. C.; Gupta, R.; Gutiérrez, R. A.; Orozco, R.; Halasa, Y. A.; Undurraga, E. A.; Hamadeh, R. R.; Hamidi, S.; Handal, A. J.; Hankey, G. J.; Hao, Y.; Harikrishnan, S.; Haro, J. M.; Hernández-Llanes, N. F.; Hoek, H. W.; Tura, A. K.; Horino, M.; Horita, N.; Hosgood, H. D.; Hoy, D. G.; Hsairi, M.; Hu, G.; Husseini, A.; Huybrechts, I.; Iburg, K. M.; Idrisov, B. T.; Kwan, G. F.; Ileanu, B. V.; Pana, A.; Kawakami, N.; Shibuya, K.; Jacobs, T. A.; Jacobsen, K. H.; Jahanmehr, N.; Jakovljevic, M. B.; Jansen, H. A. F.; Jassal, S. K.; Stein, M. B.; Javanbakht, M.; Jayaraman, S. P.; Jayatilleke, A. U.; Jee, S. H.; Jonas, J. B.; Kabir, Z.; Kalkonde, Y.; Kamal, R.; She, J.; Kan, H.; Karch, A.; Karimkhani, C.; Kaul, A.; Kazi, D. S.; Keiyoro, P. N.; Parry, C. D.; Kengne, A. P.; Matzopoulos, R.; Wiysonge, C. S.; Stein, D. J.; Mayosi, B. M.; Keren, A.; Khader, Y. S.; Khan, E. A.; Khan, G.; Khang, Y. H.; Won, S.; Khera, S.; Tavakkoli, M.; Khoja, T. A. M.; Khubchandani, J.; Kim, C.; Kim, D.; Kimokoti, R. W.; Kokubo, Y.; Koul, P. A.; Koyanagi, A.; Kravchenko, M.; Varakin, Y. Y.; Kuate, B.; Kuchenbecker, R. S.; Kucuk, B.; Kuipers, E. J.; Lallukka, T.; Shiri, R.; Meretoja, T. J.; Lan, Q.; Latif, A. A.; Lawrynowicz, A. E. B.; Leasher, J. L.; Levi, M.; Li, X.; Liang, J.; Lloyd, B. K.; Logroscino, G.; Lunevicius, R.; Pope, D.; Mahdavi, M.; Malta, D. C.; Marcenes, W.; Matsushita, K.; Nachega, J. B.; Tran, B. X.; Meaney, P. A.; Mehari, A.; Tedla, B. A.; Memish, Z. A.; Mendoza, W.; Mensink, G. B. M.; Mhimbira, F. A.; Miller, T. R.; Mills, E. J.; Mohammadi, A.; Mola, G. L. D.; Monasta, L.; Morawska, L.; Norman, R. E.; Mori, R.; Mozaff, D.; Shi, P.; Werdecker, A.; Mueller, U. O.; Paternina, A. J.; Westerman, R.;

Seedat, S.; Naheed, A.; Nangia, V.; Nassiri, N.; Nguyen, Q. L.; Nkamedjie, P. M.; Norheim, O. F.; Norrving, B.; Nyakarahuka, L.; Obermeyer, C. M.; Ogbo, F. A.; Oh, I.; Oladimeji, O.; Sartorius, B.; Olusanya, B. O.; Olivares, P. R.; Olusanya, J. O.; Opio, J. N.; Oren, E.; Ortiz, A.; Ota, E.; Mahesh, P. A.; Park, E.; Patel, T.; Patil, S. T.; Patten, S. B.; Wang, J.; Pereira, D. M.; Cortinovis, M.; Giussani, G.; Perico, N.; Remuzzi, G.; Pesudovs, K.; Phillips, M. R.; Pillay, J. D.; Plass, D.; Tobollik, M.; Polinder, S.; Pond, C. D.; Pope, C. A.; Prasad, N. M.; Qorbani, M.; Radfar, A.; Rafay, A.; Rana, S. M.; Rahman, M.; Rahman, S. U.; Rajsic, S.; Rai, R. K.; Raju, M.; Ranganathan, K.; Refaat, A. H.; Rehm, C. D.; Ribeiro, A. L.; Rojas-Rueda, D.; Roy, A.; Satpathy, M.; Tandon, N.; Rothenbacher, D.; Saleh, M. M.; Sanabria, J. R.; Sanchez-Riera, L.; Sanchez-Niño, M. D.; Sarmiento-Suarez, R.; Sawhney, M.; Schmidhuber, J.; Schneider, I. J. C.; Schutte, A. E.; Silva, D. A. S.; Shahraz, S.; Shin, M.; Shaheen, A.; Shaikh, M. A.; Sharma, R.; Shigematsu, M.; Yoon, S.; Shishani, K.; Sigfusdottir, I. D.; Singh, P. K.; Silveira, D. G. A.; Silverberg, J. I.; Yano, Y.; Soneji, S.; Stranges, S.; Steckling, N.; Sreeramareddy, C. T.; Stathopoulou, V.; Stroumpoulis, K.; Sunguya, B. F.; Swaminathan, S.; Sykes, B. L.; Tabarés-Seisdedos, R.; Talongwa, R. T.; Tanne, D.; Tuzcu, E. M.; Thakur, J.; Shaddick, G.; Thomas, M. L.; Thrift, A. G.; Thurston, G. D.; Thomson, A. J.; Topor-Madry, R.; Topouzis, F.; Towbin, J. A.; Uthman, O. A.; Tobe-Gai, R.; Tsilimparis, N.; Tsala, Z.; Tyrovolas, S.; Ukwaja, K. N.; van Os, J.; Vasankari, T.; Venketasubramanian, N.; Violante, F. S.; Waller, S. G.; Uneke, C. J.; Wang, Y.; Weichenthal, S.; Woolf, A. D.; Xavier, D.; Xu, G.; Yakob, B.; Yip, P.; Kesavachandran, C. N.; Montico, M.; Ronfani, L.; Yu, C.; Zaidi, Z.; Yonemoto, N.; Younis, M. Z.; Wubshet, M.; Zuhlke, L. J.; Zaki, M. E.; Zhu, J. Global, Regional, and National Comparative Risk Assessment of 79 Behavioural, Environmental and Occupational, and Metabolic Risks or Clusters of Risks, 1990–2015: A Systematic Analysis for the Global Burden of Disease Study 2015. *Lancet* **2016**, *388* (10053), 1659–1724. https://doi.org/10.1016/S0140-6736(16)31679-8.

(7) Lelieveld, J.; Evans, J. S.; Fnais, M.; Giannadaki, D.; Pozzer, A. The Contribution of Outdoor Air Pollution Sources to Premature Mortality on a Global Scale. *Nature* **2015**, *525* (7569), 367–371. https://doi.org/10.1038/nature15371.

(8) Burnett, R.; Chen, H.; Szyszkowicz, M.; Fann, N.; Hubbell, B.; Pope, C. A.; Apte, J. S.; Brauer, M.; Cohen, A.; Weichenthal, S.; Coggins, J.; Di, Q.; Brunekreef, B.; Frostad, J.; Lim, S. S.; Kan, H.; Walker, K. D.; Thurston, G. D.; Hayes, R. B.; Lim, C. C.; Turner, M. C.; Jerrett, M.; Krewski, D.; Gapstur, S. M.; Diver, W. R.; Ostro, B.; Goldberg, D.; Crouse, D. L.; Martin, R. V.; Peters, P.; Pinault, L.; Tjepkema, M.; Van Donkelaar, A.; Villeneuve, P. J.; Miller, A. B.; Yin, P.; Zhou, M.; Wang, L.; Janssen, N. A. H.; Marra, M.; Atkinson, R. W.; Tsang, H.; Thach, T. Q.; Cannon, J. B.; Allen, R. T.; Hart, J. E.; Laden, F.; Cesaroni, G.; Forastiere, F.; Weinmayr, G.; Jaensch, A.; Nagel, G.; Concin, H.; Spadaro, J. V. Global Estimates of Mortality Associated with Longterm Exposure to

633 Outdoor Fine Particulate Matter. *Proc. Natl. Acad. Sci. U. S. A.* **2018**, *115* (38), 9592–
634 9597. https://doi.org/10.1073/pnas.1803222115.

635 (9) Müller, A.; Österlund, H.; Marsalek, J.; Viklander, M. The Pollution Conveyed by Urban
636 Runoff: A Review of Sources. *Science of the Total Environment*. Elsevier B.V. March 20,
637 2020, p 136125. https://doi.org/10.1016/j.scitotenv.2019.136125.

638 (10) Levin, P. S.; Howe, E.; Robertson, J. C. Impacts of Stormwater on Coastal Ecosystems:
639 The Need to Match the Scales of Management Objectives and Solutions. *Philos. Trans. R.*
640 *Soc. London B.* **2020**, *in press*.

641 (11) Yeh, S.; Mishra, G. S.; Fulton, L.; Kyle, P.; McCollum, D. L.; Miller, J.; Cazzola, P.;
642 Teter, J. Detailed Assessment of Global Transport-Energy Models' Structures and
643 Projections. *Transp. Res. Part D Transp. Environ.* **2017**, *55*, 294–309.
644 https://doi.org/10.1016/j.trd.2016.11.001.

645 (12) Jayarathne, A.; Egodawatta, P.; Ayoko, G. A.; Goonetilleke, A. Assessment of Ecological
646 and Human Health Risks of Metals in Urban Road Dust Based on Geochemical
647 Fractionation and Potential Bioavailability. *Sci. Total Environ.* **2018**, *635*, 1609–1619.
648 https://doi.org/10.1016/J.SCITOTENV.2018.04.098.

649 (13) Chen, L. C.; Lippmann, M. Effects of Metals within Ambient Air Particulate Matter (PM)
650 on Human Health. *Inhal. Toxicol.* **2009**, *21* (1), 1–31.
651 https://doi.org/10.1080/08958370802105405.

652 (14) Caussy, D.; Gochfeld, M.; Gurzau, E.; Neagu, C.; Ruedel, H. Lessons from Case Studies
653 of Metals: Investigating Exposure, Bioavailability, and Risk. *Ecotoxicol. Environ. Saf.*
654 **2003**, *56* (1), 45–51. https://doi.org/10.1016/S0147-6513(03)00049-6.

655 (15) Ma, Y.; McGree, J.; Liu, A.; Deilami, K.; Egodawatta, P.; Goonetilleke, A. Catchment
656 Scale Assessment of Risk Posed by Traffic Generated Heavy Metals and Polycyclic
657 Aromatic Hydrocarbons. *Ecotoxicol. Environ. Saf.* **2017**, *144*, 593–600.
658 https://doi.org/10.1016/J.ECOENV.2017.06.073.

659 (16) Liu, A.; Ma, Y.; Gunawardena, J. M. A.; Egodawatta, P.; Ayoko, G. A.; Goonetilleke, A.
660 Heavy Metals Transport Pathways: The Importance of Atmospheric Pollution
661 Contributing to Stormwater Pollution. *Ecotoxicol. Environ. Saf.* **2018**, *164*, 696–703.
662 https://doi.org/10.1016/j.ecoenv.2018.08.072.

663 (17) McKenzie, E. R.; Money, J. E.; Green, P. G.; Young, T. M. Metals Associated with
664 Stormwater-Relevant Brake and Tire Samples. *Sci. Total Environ.* **2009**, *407* (22), 5855–
665 5860. https://doi.org/10.1016/J.SCITOTENV.2009.07.018.

666 (18) Thorpe, A.; Harrison, R. M. Sources and Properties of Non-Exhaust Particulate Matter
667 from Road Traffic: A Review. *Sci. Total Environ.* **2008**, *400* (1–3), 270–282.

https://doi.org/10.1016/j.scitotenv.2008.06.007.

(19) Davis, A. P.; Shokouhian, M.; Ni, S. Loading Estimates of Lead, Copper, Cadmium, and Zinc in Urban Runoff from Specific Sources. *Chemosphere* **2001**, *44* (5), 997–1009. https://doi.org/10.1016/S0045-6535(00)00561-0.

(20) Zhang, K.; Chui, T. F. M. A Comprehensive Review of Spatial Allocation of LID-BMP-GI Practices: Strategies and Optimization Tools. *Sci. Total Environ.* **2018**, *621*, 915–929. https://doi.org/10.1016/J.SCITOTENV.2017.11.281.

(21) Barzyk, T. M.; Isakov, V.; Arunachalam, S.; Venkatram, A.; Cook, R.; Naess, B. A Near-Road Modeling System for Community-Scale Assessments Oftraffic-Related Air Pollution in the United States. *Environ. Model. Softw.* **2015**, *66*, 46–56. https://doi.org/10.1016/j.envsoft.2014.12.004.

(22) Zivkovich, B. R.; Mays, D. C. Predicting Nonpoint Stormwater Runoff Quality from Land Use. *PLoS One* **2018**, *13* (5), e0196782. https://doi.org/10.1371/journal.pone.0196782.

(23) Mitchell, G. Mapping Hazard from Urban Non-Point Pollution: A Screening Model to Support Sustainable Urban Drainage Planning. *Journal of Environmental Management*. Academic Press January 1, 2005, pp 1–9. https://doi.org/10.1016/J.JENVMAN.2004.08.002.

(24) Ma, J. S.; Kang, J. H.; Kayhanian, M.; Stenstrom, M. K. Sampling Issues in Urban Runoff Monitoring Programs: Composite versus Grab. *J. Environ. Eng.* **2009**, *135* (3), 118–127. https://doi.org/10.1061/(ASCE)0733-9372(2009)135:3(118).

(25) Hennigan, C. J.; Mucci, A.; Reed, B. E. Trends in PM 2.5 Transition Metals in Urban Areas across the United States. *Environ. Res. Lett.* **2019**, *14* (10), 104006. https://doi.org/10.1088/1748-9326/ab4032.

(26) Dabek-Zlotorzynska, E.; Dann, T. F.; Kalyani Martinelango, P.; Celo, V.; Brook, J. R.; Mathieu, D.; Ding, L.; Austin, C. C. Canadian National Air Pollution Surveillance (NAPS) PM2.5 Speciation Program: Methodology and PM2.5 Chemical Composition for the Years 2003-2008. *Atmos. Environ.* **2011**, *45* (3), 673–686. https://doi.org/10.1016/j.atmosenv.2010.10.024.

(27) Philip, S.; Martin, R. V.; Van Donkelaar, A.; Lo, J. W. H.; Wang, Y.; Chen, D.; Zhang, L.; Kasibhatla, P. S.; Wang, S.; Zhang, Q.; Lu, Z.; Streets, D. G.; Bittman, S.; Macdonald, D. J. Global Chemical Composition of Ambient Fine Particulate Matter for Exposure Assessment. *Environ. Sci. Technol.* **2014**, *48* (22), 13060–13068. https://doi.org/10.1021/es502965b.

(28) Gatziolis, D.; Jovan, S.; Donovan, G.; Amacher, M. *Elemental Atmospheric Pollution Assessment Via Moss-Based Measurements in Portland, Oregon. General Technical*

Report PNW-GTR-938.; 2016; Vol. 938.

(29) Jiang, Y.; Fan, M.; Hu, R.; Zhao, J.; Wu, Y. Mosses Are Better than Leaves of Vascular Plants in Monitoring Atmospheric Heavy Metal Pollution in Urban Areas. *Int. J. Environ. Res. Public Health* **2018**. https://doi.org/10.3390/ijerph15061105.

(30) Ruckelshaus, M.; Essington, T.; Levin, P. Puget Sound, Washington, USA. In *Ecosystem-based Management for the Oceans*; McLeod, K., Leslie, H., Eds.; Island Press: Washington, DC, USA: Washington, D.C., 2009; pp 201–226.

(31) Zechmeister, H. G.; Hohenwallner, D.; Riss, A.; Hanus-Illnar, A. Estimation of Element Deposition Derived from Road Traffic Sources by Using Mosses. *Environ. Pollut.* **2005**, *138* (2), 238–249. https://doi.org/10.1016/j.envpol.2005.04.005.

(32) Horstmeyer, N.; Huber, M.; Drewes, J. E.; Helmreich, B. Evaluation of Site-Specific Factors Influencing Heavy Metal Contents in the Topsoil of Vegetated Infiltration Swales. *Sci. Total Environ.* **2016**, *560–561*, 19–28. https://doi.org/10.1016/j.scitotenv.2016.04.051.

(33) Apeagyei, E.; Bank, M. S.; Spengler, J. D. Distribution of Heavy Metals in Road Dust along an Urban-Rural Gradient in Massachusetts. *Atmos. Environ.* **2011**, *45* (13), 2310–2323. https://doi.org/10.1016/J.ATMOSENV.2010.11.015.

(34) Pasquier, A.; André, M. Considering Criteria Related to Spatial Variabilities for the Assessment of Air Pollution from Traffic. *Transp. Res. Procedia* **2017**, *25*, 3354–3369. https://doi.org/10.1016/J.TRPRO.2017.05.210.

(35) Gunawardena, J. M. A.; Liu, A.; Egodawatta, P.; Ayoko, G. A.; Goonetilleke, A. Primary Traffic Related Pollutants and Urban Stormwater Quality; Springer, Singapore, 2018; pp 1–16. https://doi.org/10.1007/978-981-10-5302-3_1.

(36) Deforest, D. K.; Meyer, J. S. Critical Review: Toxicity of Dietborne Metals to Aquatic Organisms. *Critical Reviews in Environmental Science and Technology*. June 3, 2015, pp 1176–1241. https://doi.org/10.1080/10643389.2014.955626.

(37) Gunawardena, J. M. A.; Egodawatta, P.; Ayoko, G. A.; Goonetilleke, A. Atmospheric Deposition as a Source of Heavy Metals in Urban Stormwater. *Atmos. Environ.* **2013**, *68*, 235–242. https://doi.org/10.1016/j.atmosenv.2012.11.062.

(38) Duong, T. T. T.; Lee, B. K. Determining Contamination Level of Heavy Metals in Road Dust from Busy Traffic Areas with Different Characteristics. *J. Environ. Manage.* **2011**, *92* (3), 554–562. https://doi.org/10.1016/j.jenvman.2010.09.010.

(39) Puget Sound Regional Council. *2050 Forecast of People and Jobs*; Puget Sound Regional Council: Seattle Washington, 2018.

(40) Mathews, D. L.; Turner, N. J. Ocean Cultures: Northwest Coast Ecosystems and Indigenous Management Systems. In *Conservation for the Antropocene Ocean: Interdisciplinary science in support of nature and people*; Levin, P. S., Poe, M. R., Eds.; Academic Press: London, 2017; pp 169–206.

(41) Yang, L.; Jin, S.; Danielson, P.; Homer, C.; Gass, L.; Bender, S. M.; Case, A.; Costello, C.; Dewitz, J.; Fry, J.; Funk, M.; Granneman, B.; Liknes, G. C.; Rigge, M.; Xian, G. A New Generation of the United States National Land Cover Database: Requirements, Research Priorities, Design, and Implementation Strategies. *ISPRS J. Photogramm. Remote Sens.* **2018**, *146*, 108–123. https://doi.org/10.1016/J.ISPRSJPRS.2018.09.006.

(42) Tostes, A. I. J.; de L. P. Duarte-Figueiredo, F.; Assunção, R.; Salles, J.; Loureiro, A. A. F. From Data to Knowledge: City-Wide Traffic Flows Analysis and Prediction Using Bing Maps. *Proc. 2nd ACM SIGKDD Int. Work. Urban Comput. - UrbComp '13* **2013**, 1–8. https://doi.org/10.1145/2505821.2505831.

(43) Little, P.; Martin, M. H. Biological Monitoring of Heavy Metal Pollution. *Environ. Pollut.* **1974**, *6* (1), 1–19. https://doi.org/10.1016/0013-9327(74)90042-1.

(44) Fernández, J. A.; Boquete, M. T.; Carballeira, A.; Aboal, J. R. A Critical Review of Protocols for Moss Biomonitoring of Atmospheric Deposition: Sampling and Sample Preparation. *Science of the Total Environment*. Elsevier June 1, 2015, pp 132–150. https://doi.org/10.1016/j.scitotenv.2015.02.050.

(45) Bates, J. W. Mineral Nutrient Acquisition and Retention by Bryophytes. *J. Bryol.* **1992**, *17* (2), 223–240. https://doi.org/10.1179/jbr.1992.17.2.223.

(46) Aboal, J. R.; Pérez-Llamazares, A.; Carballeira, A.; Giordano, S.; Fernández, J. A. Should Moss Samples Used as Biomonitors of Atmospheric Contamination Be Washed? *Atmos. Environ.* **2011**, *45* (37), 6837–6840. https://doi.org/10.1016/j.atmosenv.2011.09.004.

(47) Salemaa, M.; Derome, J.; Helmissari, H.; Nieminen, T.; Vanhamajamaa, I. Element Accumulation in Boreal Bryophytes, Lichens and Vascular Plants Exposed to Heavy Metal and Sulfur Deposition in Finland. *Sci. Total Environ.* **2004**, *324* (1–3), 141–160. https://doi.org/10.1016/j.scitotenv.2003.10.025.

(48) Pearson, J.; Wells, D. M.; Seller, K. J.; Bennett, A.; Soares, A.; Woodall, J.; Ingrouille, M. J. Traffic Exposure Increases Natural 15N and Heavy Metal Concentrations in Mosses. *New Phytol.* **2000**, *147*, 317–326.

(49) Kalnicky, D. J.; Singhvi, R. Field Portable XRF Analysis of Environmental Samples. *J. Hazard. Mater.* **2001**, *83* (1–2), 93–122. https://doi.org/10.1016/S0304-3894(00)00330-7.

(50) United States Environmental Protection Agency. *Field Portable X-Ray Fluorescence Spectrometry for the Determination of Elemental Concentrations in Soil and Sediment*;

2007.

(51) Towett, E. K.; Shepherd, K. D.; Lee Drake, B. Plant Elemental Composition and Portable X-Ray Fluorescence (PXRF) Spectroscopy: Quantification under Different Analytical Parameters. *X-Ray Spectrom.* **2016**, *45* (2), 117–124. https://doi.org/10.1002/xrs.2678.

(52) Bueno Guerra, M. B.; de Almeida, E.; Carvalho, G. G. A.; Souza, P. F.; Nunes, L. C.; Júnior, D. S.; Krug, F. J. Comparison of Analytical Performance of Benchtop and Handheld Energy Dispersive X-Ray Fluorescence Systems for the Direct Analysis of Plant Materials. *J. Anal. At. Spectrom.* **2014**, *29* (9), 1667–1674. https://doi.org/10.1039/C4JA00083H.

(53) Aboal, J. R.; Fernández, J. A.; Boquete, T.; Carballeira, A. Is It Possible to Estimate Atmospheric Deposition of Heavy Metals by Analysis of Terrestrial Mosses? *Science of the Total Environment*. 2010, pp 6291–6297. https://doi.org/10.1016/j.scitotenv.2010.09.013.

(54) Kuhn, M.; Johnson, K. *Applied Predictive Modeling*; Springer New York, 2013. https://doi.org/10.1007/978-1-4614-6849-3.

(55) Markert, B.; Weckert, V. Use of Polytrichum Formosum (Moss) as a Passive Biomonitor for Heavy Metal Pollution (Cadmium, Copper, Lead and Zinc). *Sci. Total Environ.* **1989**, *86* (3), 289–294. https://doi.org/10.1016/0048-9697(89)90291-X.

(56) Real, C.; Fernández, J. A.; Aboal, J. R.; Carballeira, A. Detection of Pulses of Atmospheric Mercury Deposition with Extensive Surveys and Frequently Sampled Stations: A Comparison. *Ecotoxicol. Environ. Saf.* **2008**, *70* (3), 392–399. https://doi.org/10.1016/J.ECOENV.2008.01.005.

(57) Boquete, M. T.; Fernández, J. A.; Aboal, J. R.; Carballeira, A. Analysis of Temporal Variability in the Concentrations of Some Elements in the Terrestrial Moss Pseudoscleropodium Purum. *Environ. Exp. Bot.* **2011**, *72* (2), 210–216. https://doi.org/10.1016/j.envexpbot.2011.03.002.

(58) Bivand, R.; with contributions by; Anselin, L.; Assunção, R.; Berke, O.; Bernat, A.; Carvalho, M.; Chun, Y.; Christensen, B.; Dormann, C.; Dray, S.; Halbersma, R.; Krainski, E.; Lewin-Koh, N.; Li, H.; Ma, J.; Millo, G.; Mueller, W.; Ono, H.; Peres-Neto, P.; Reder, M.; Tiefelsdorf, M.; Yu, D. The Spdep Package - Spatial Dependence: Weighting Schemes, Statistics and Models. 2009, p 163.

(59) Porter, W. C.; Heald, C. L.; Cooley, D.; Russell, B. Investigating the Observed Sensitivities of Air-Quality Extremes to Meteorological Drivers via Quantile Regression. *Atmos. Chem. Phys.* **2015**, *15* (18), 10349–10366. https://doi.org/10.5194/acp-15-10349-2015.

(60) Pant, P.; Harrison, R. M. Estimation of the Contribution of Road Traffic Emissions to Particulate Matter Concentrations from Field Measurements: A Review. *Atmospheric Environment*. Pergamon October 1, 2013, pp 78–97. https://doi.org/10.1016/j.atmosenv.2013.04.028.

(61) Tong, Z.; Whitlow, T. H.; MacRae, P. F.; Landers, A. J.; Harada, Y. Quantifying the Effect of Vegetation on Near-Road Air Quality Using Brief Campaigns. *Environ. Pollut.* **2015**, *201*, 141–149. https://doi.org/10.1016/J.ENVPOL.2015.02.026.

(62) De Miguel, E.; Llamas, J. F.; Chacón, E.; Berg, T.; Larssen, S.; Røyset, O.; Vadset, M. Origin and Patterns of Distribution of Trace Elements in Street Dust: Unleaded Petrol and Urban Lead. *Atmos. Environ.* **1997**, *31* (17), 2733–2740. https://doi.org/10.1016/S1352-2310(97)00101-5.

(63) Schwarz, K.; Pickett, S. T. A.; Lathrop, R. G.; Weathers, K. C.; Pouyat, R. V.; Cadenasso, M. L. The Effects of the Urban Built Environment on the Spatial Distribution of Lead in Residential Soils. *Environ. Pollut.* **2012**, *163*, 32–39. https://doi.org/10.1016/j.envpol.2011.12.003.

(64) Wijesiri, B.; Liu, A.; Gunawardana, C.; Hong, N.; Zhu, P.; Guan, Y.; Goonetilleke, A. Influence of Urbanisation Characteristics on the Variability of Particle-Bound Heavy Metals Build-up: A Comparative Study between China and Australia. *Environ. Pollut.* **2018**, *242*, 1067–1077. https://doi.org/10.1016/J.ENVPOL.2018.07.123.

(65) Rouillon, M.; Gore, D. B.; Taylor, M. P. The Nature and Distribution of Cu, Zn, Hg, and Pb in Urban Soils of a Regional City: Lithgow, Australia. *Appl. Geochemistry* **2013**, *36*, 83–91. https://doi.org/10.1016/j.apgeochem.2013.06.015.

(66) Li, H.; Shi, A.; Zhang, X. Particle Size Distribution and Characteristics of Heavy Metals in Road-Deposited Sediments from Beijing Olympic Park. *J. Environ. Sci. (China)* **2015**, *32*, 228–237. https://doi.org/10.1016/j.jes.2014.11.014.

(67) Hou, D.; O'Connor, D.; Nathanail, P.; Tian, L.; Ma, Y. Integrated GIS and Multivariate Statistical Analysis for Regional Scale Assessment of Heavy Metal Soil Contamination: A Critical Review. *Environ. Pollut.* **2017**, *231*, 1188–1200. https://doi.org/10.1016/J.ENVPOL.2017.07.021.

(68) Gunawardena, J. M. A.; Ziyath, A. M.; Egodawatta, P.; Ayoko, G. A.; Goonetilleke, A. Sources and Transport Pathways of Common Heavy Metals to Urban Road Surfaces. *Ecol. Eng.* **2015**, *77*, 98–102. https://doi.org/10.1016/J.ECOLENG.2015.01.023.

(69) Schröder, W.; Holy, M.; Pesch, R.; Harmens, H.; Ilyin, I.; Steinnes, E.; Alber, R.; Aleksiayenak, Y.; Blum, O.; Coşkun, M.; Dam, M.; De Temmerman, L.; Frolova, M.; Frontasyeva, M.; Miqueo, L. G.; Grodzińska, K.; Jeran, Z.; Korzekwa, S.; Krmar, M.;

Kubin, E.; Kvietkus, K.; Leblond, S.; Liiv, S.; Magnússon, S.; Maňkovská, B.; Piispanen, J.; Rühling, Å.; Santamaria, J.; Spiric, Z.; Suchara, I.; Thöni, L.; Urumov, V.; Yurukova, L.; Zechmeister, H. G. Are Cadmium, Lead and Mercury Concentrations in Mosses across Europe Primarily Determined by Atmospheric Deposition of These Metals? *J. Soils Sediments* **2010**, *10* (8), 1572–1584. https://doi.org/10.1007/s11368-010-0254-y.

(70) Barrington-Leigh, C.; Millard-Ball, A. The World's User-Generated Road Map Is More than 80% Complete. *PLoS One* **2017**, *12* (8), e0180698. https://doi.org/10.1371/journal.pone.0180698.

(71) Microsoft. Bing Maps Traffic Coverage https://docs.microsoft.com/en-us/bingmaps/coverage/traffic-coverage-old.

(72) Winkler, A.; Contardo, T.; Vannini, A.; Sorbo, S.; Basile, A.; Loppi, S. Magnetic Emissions from Brake Wear Are the Major Source of Airborne Particulate Matter Bioaccumulated by Lichens Exposed in Milan (Italy). *Appl. Sci.* **2020**. https://doi.org/10.3390/app10062073.

(73) Bukowiecki, N.; Lienemann, P.; Hill, M.; Figi, R.; Richard, A.; Furger, M.; Rickers, K.; Falkenberg, G.; Zhao, Y.; Cliff, S. S.; Prevot, A. S. H.; Baltensperger, U.; Buchmann, B.; Gehrig, R. Real-World Emission Factors for Antimony and Other Brake Wear Related Trace Elements: Size-Segregated Values for Light and Heavy Duty Vehicles. *Environ. Sci. Technol.* **2009**. https://doi.org/10.1021/es9006096.